Original scientific paper

Informacije MIDEM
Journal of Microelectronics,
Electronic Components and Materials
Vol. 47, No. 2(2017), 71 – 78

$Pb(Mg,Nb)O_3$–$PbTiO_3$ thick films on metalized low-temperature co-fired ceramic substrates

H. Uršič[1], A. Benčan[1,2], E. Khomyakova[1], S. Drnovšek[1], I. F. Mercioniu[3], K. Makarovič[1,2,4], D. Belavič[5], C. Schreiner[6], R. Ciobanu[6], P. Fanjul Bolado[7], B. Malič[1]

[1]*Jožef Stefan Institute, Ljubljana, Slovenia*
[2]*Centre of Excellence NAMASTE, Ljubljana, Slovenia*
[3]*Institutul National Cercetare-Dezvoltare pentru Fizica Materialelor, Bucharest, Romaina*
[4]*Keko Equipment Ltd., Žužemberk, Slovenia*
[5]*HIPOT-RR d.o.o., Otočec, Slovenia*
[6]*Technical University of Iasi, Iasi, Romania*
[7]*DROPSENS, Parque Tecnológico de Asturias - Llanera, Spain*

Abstract: Compatibility of screen-printed piezoelectric $0.65Pb(Mg_{1/3}Nb_{2/3})O_3$–$0.35PbTiO_3$ thick films with metalized low-temperature co-fired (LTCC) ceramic substrates is examined. Such substrates are interesting for micro-electro mechanical systems, for example for piezoelectric sensors and actuators, where functional layers are usually Pb-based piezoelectrics. In this study the special attention is given to the influence of the Au, Ag and Ag/Pd electrode materials coated over the LTCC on the functional properties of the films. The best phase purity, dielectric and piezoelectric properties were obtained in the films on gilded substrates. No secondary phases were observed at the film/Au interface by scanning electron microscope. The piezoelectric coefficient d_{33} of the films on gilded substrates is equal to 120 pC/N.

Keywords: PMN-PT; piezoelectric; thick film; domain structure; low-temperature co-fired ceramic; LTCC

Debele plasti $Pb(Mg,Nb)O_3$–$PbTiO_3$ na podlagah iz keramike z nizko temperature žganja

Izvleček: V članku poročamo o pripravi piezoelektričnih $0{,}65Pb(Mg_{1/3}Nb_{2/3})O_3$–$0{,}35PbTiO_3$ debelih plasti na podlagah iz keramike z nizko temperature žganja. Omenjene podlage so uporabne v mikro elektro mehanskih sistemih, kot so piezoelektrični senzorji in aktuatorji, zato je njihova kompatibilnost s funkcijskimi plastmi velikega pomena. Preučevali smo vpliv spodnje elektrode na lastnosti funkcijskih plasti. Pripravili smo vzorce s tremi različnimi elektrodami, z Ag, Ag/Pd in Au. Ugotovili smo, da plasti na različnih elektrodah izkazujejo različno fazno sestavo, dielektrične in piezoelektrične lastnosti. Plasti na Au elektrodah izkazujejo veliko boljše dielektrične in piezoelektrične lastnosti ter vsebujejo manj sekundarnih faz kot plasti na Ag in Ag/Pd elektrodah. Piezoelektrični koeficient d_{33} plasti na podlagah iz keramike z nizko temperaturo žganja z zlatimi elektrodami je 120 pC/N.

Ključne besede: PMN-PT; piezoelektrik; debela plast; domenska struktura; keramika z nizko temperaturo žganja, LTCC

** Corresponding Author's e-mail: hana.ursic@ijs.si*

1 Introduction

The thick-film technology is attractive for the production of simple functional structures and also quite complex systems. Screen-printing is one of the most widely used thick-film deposition techniques for producing up to a hundred micrometres thick piezoelectric films. Commercially available piezoelectric thick films are mostly based on $Pb(Zr,Ti)O_3$ solid solution [1]. The most commonly used substrate materials for piezoelectric ceramic thick films are silicon and alumina. However, low-temperature co-fired ceramics (LTCC) are promising for the fabrication of three-dimensional ceramic

structures or ceramic micro-electro-mechanical systems (c-MEMS) and for this reason considered as desirable substrates for functional layers. The LTCC are based on glass-ceramic composites or crystallizing glass and densify at relatively low temperature (around 850 °C), which enables the use of low cost conductive materials and fast firing profiles [2, 3]. Therefore the LTCC and thick-film technologies enable fast and easy fabrication of electronic devices and systems, which could reduce the cost of devices and shorten the time of fabrication [2, 4]. The LTCC materials are especially interesting for actuator and sensor applications due to lower Young's modulus (90–110 GPa) than alumina (210–410 GPa), which enables high actuation sensitivity [1].

An alternative to $Pb(Zr,Ti)O_3$-based piezoelectric material is $(1-x)Pb(Mg_{1/3}Nb_{2/3})O_3–xPbTiO_3$ (PMN–100*x*PT) solid solution with the morphotropic phase boundary at $x = 0.35$ [5, 6]. The PMN–35PT thick films prepared on silicon and alumina substrates possesses high dielectric permittivity (more than 3000 at 1 kHz and room temperature [7-9]) and high piezoelectric coefficients (d_{33} of 150 to 200 pC/N [9, 10]), and are therefore promising for sensor and actuator applications [11].

The aim of this work was to examine the compatibility of PMN–35PT piezoelectric thick films with metalized LTCC substrates. Until recently, only the $Pb(Zr,Ti)O_3$-based piezoelectric thick films were processed on LTCC substrates [12-15]. But, the glass phase from LTCC may interact with $PbZr_{0.53}Ti_{0.47}O_3$ (PZT) thick film and PbO from the thick film may diffuse into the LTCC during annealing [12, 13], which leads to changes in the thick film's phase composition and consequently functional properties. Hence the processing of piezoceramic films on LTCC materials is still challenging. In order to prevent the film-substrate interactions different solutions were reported, such as interposing of the barrier layer [12] or use of a very dense Au bottom electrode [15]. In this work the PMN–35PT thick films were prepared on metalized LTCC substrates with the interposed 15 µm thick PZT barrier layer to minimize the film-substrate interactions.

2 Experimental methods

For the synthesis of the PMN–35PT powder, PbO (99.9 %, Aldrich), MgO (98 %, Aldrich), TiO_2 (99.8 %, Alfa Aesar) and Nb_2O_5 (99.9 %, Aldrich) were used. A mixture of these oxides in the molar ratio corresponding to the PMN–35PT stoichiometry with an excess of 2 mol% PbO was high-energy milled for 72 h at 300 rpm in a Retsch Model PM 400 planetary mill, and additionally in an attritor mill for 4 h at 800 rpm in isopropanol. The powder was then heated at 700 °C for 1 h. The size of the particles after heating was determined by a light-scattering technique using a Microtrac S3500 Series Particle Size Analyzer instrument. The results were derived from the area particle size distribution. The most common parameter used is the median particle size d_{50}, where the area of all particles smaller than d_{50} accounts for 50 % of the area of all the particles. The powder morphology was analysed using the field-emission scanning electron microscopy (FE-SEM) JSM 7600F (Jeol, Tokyo, Japan). The powders were dispersed in acetone under ultrasound, and a few drops were spread on highly oriented pyrolytic graphite substrates. The PMN–35PT thick-film paste was prepared from a mixture of the PMN–35PT powder and an organic vehicle consisting of alpha-terpineol, [2-(2-butoxy-ethoxy)-ethyl]-acetate and ethyl cellulose in the ratio 60/25/15. For more details on PMN–35PT powder and thick-film paste processing and characterization see [7, 16].

The LTCC substrates were prepared by laminating three layers of the LTCC tape (DuPont 951) at 50 °C and 20 MPa. The laminated tapes were than heated at 450 °C for 1 h to burn-out the organic binder and densified at 875 °C for 15 min. In order to minimize the chemical interactions between the PMN–35PT thick film and the LTCC substrate, a PZT barrier layer was interposed between substrate and bottom electrode as suggested in [7, 17]. The PZT thick-film paste was printed on substrate and sintered 870 °C for 1 h. For more details regarding PZT powder and thick-film paste processing see [7]. The PZT/LTCC structure is further-on referred as the substrate. Thick-film silver (Ag ESL 9912MM), silver/palladium (80Ag/20Pd FERRO EL44-001) and gold (Au ESL 8884G) conductors were printed on the barrier layer/substrate structures and fired at 850 °C for 1 h. The thicknesses of the sintered electrodes were 50, 25 and 25 µm, respectively.

The PMN–35PT paste was printed five times on the electrode substrate with intermediate drying at 150 °C after each printing step. The samples were pressed at 50 MPa, heated at 500 °C for 1 h to decompose the organic vehicle [16], sintered at 850 °C for 2 h in covered alumina crucibles in the presence of $PbZrO_3$ packing powder with an excess of 2 mol% PbO and then cooled to room temperature with a rate of 2 °C/min.

The X-ray diffraction (XRD) patterns of the films were recorded using a PANalytical X'Pert PRO MPD (X'Pert PRO MPD, PANalytical, Almeo, The Netherlands) diffractometer with Cu–Kα1 radiation. The XRD patterns were recorded in the 2θ region from 10° to 70° using a detector with a capture angle of 2.122°. The exposure time for each step was 100 s and the interval between the obtained data points was 0.034°.

For microstructural analysis the samples were mounted in epoxy, ground and polished using standard metallographic techniques. The microstructures of the samples were investigated with a FE-SEM JSM 7600F (Jeol, Tokyo, Japan) equipped with an Inca Energy Detector. The energy-dispersive X-ray spectroscopy (EDXS) analyses were performed at 15 keV. The average grain size (GS) was estimated from the SEM images obtained by backscattered electrons (BE) of the film's surface. For the stereological analysis more than 400 grains per sample were measured with the Image Tool Software. The GS is expressed as the Feret's diameter.

The topography and piezoresponse images were recorded with an atomic force microscope (AFM; Asylum Research, Molecular Force Probe 3D, Santa Barbara, CA, USA) equipped with a piezoresponse force mode (PFM). A tetrahedral Si tip coated with Ti/Ir (Asyelec-01, Atomic-Force F&E GmbH, Mannheim, Germany) with the curvature diameter of 30 nm ± 10 nm was applied for scanning the sample surface. The out-of-plane amplitude PFM images were measured in the Single mode at ac amplitude signal of 20 V and frequency of ~300 kHz. The local amplitude and phase hysteresis responses were measured in the Dual AC Resonance Tracking Switching Spectroscopy (DART-SS) mode with the waveform parameters: increasing step signal with maximum amplitude of 60 V and frequency 0.1 Hz; overlapping sinusoidal signal of amplitude 5 V and frequency 20 Hz, off-loop mode.

For dielectric and piezoelectric measurements, Cr/Au electrodes with a 1.5-mm diameter were deposited on the top surface of the films using RF-magnetron sputtering (5 Pascal). The dielectric permittivity (ε`) and dielectric losses (tan δ) versus temperature were measured with a HP 4284 A Precision LCR Meter by ac amplitude of 1 V and frequencies of 1, 10, and 100 kHz during cooling from 300 °C to 25 °C. The films were poled at 160 °C with a dc electric field from 2.5 to 7.5 kV/mm for 5 min and field-cooled to 25 °C. After poling the samples were aged for 24 h. The piezoelectric constants d_{33} were measured by Berlincourt piezometer (Take Control PM10, Birmingham, UK) at alternating stress frequency of 100 Hz.

3 Results and discussion

3.1 Characterisation of PMN–35PT powder

The particle size distribution of the PMN–35PT powder used for preparation of the thick-film paste is shown in Figure 1(a). The d_{50} was 0.32 µm. Around 10 % of the particles are larger than 1 µm, while the majority of them has a sub-micrometre size. Such distribution was confirmed by the FE-SEM analysis, where both fine submicrometre and coarse particles were observed (Figure 1(b)). The XRD pattern of PMN–35PT mechanochemically synthesized powder after calcination at 700 °C is shown in Figure 1(c). All reflections correspond to the perovskite phase.

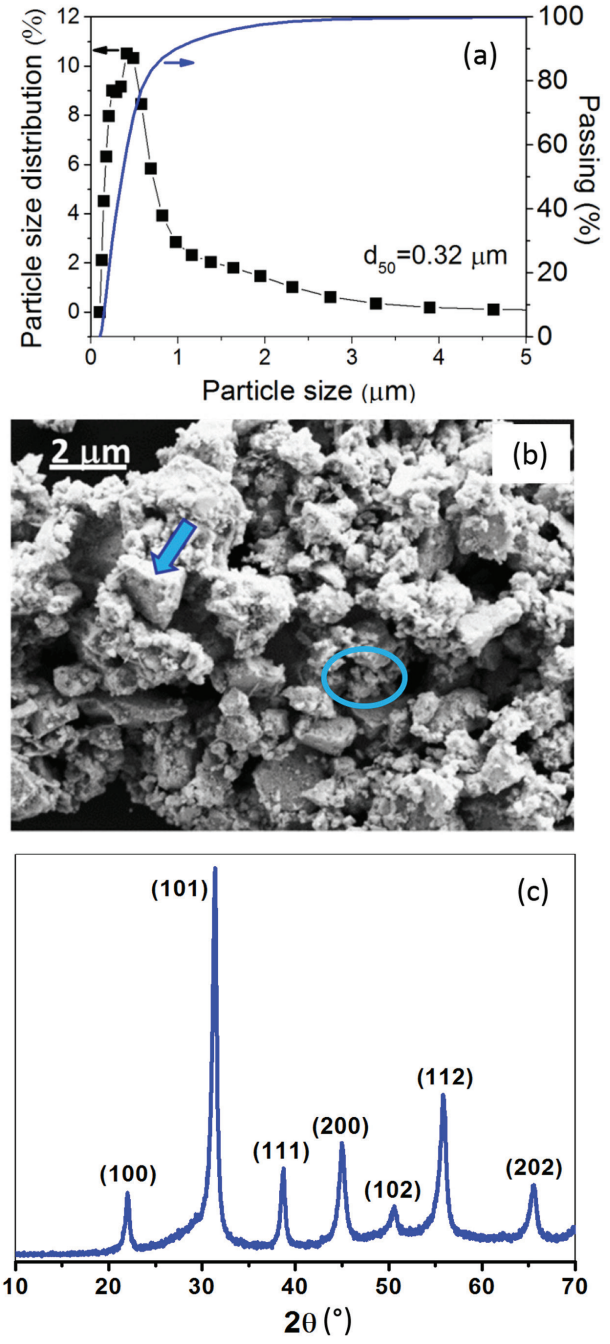

Figure 1: (a) The area particle size distribution, (b) FE-SEM micrograph and (c) XRD pattern of the PMN–35PT powder after heating at 700 °C for 1 h. A coarse particle and smaller, submicron sized particles are marked by an arrow and a circle in panel (b), respectively. The indexed peaks of the pseudo-cubic perovskite phase (JCPDS 81-0861) are shown in brackets in panel (c).

3.2 The influence of the bottom electrode material on the phase composition and functional properties of PMN–35PT films

In order to study the influence of the bottom electrode layer on the properties of functional thick-film structures three different electrode materials were used; Ag, Ag/Pd and Au. Corresponding XRD patterns of ~60 µm thick PMN–35PT films on the metalized substrates are shown in Figure 2.

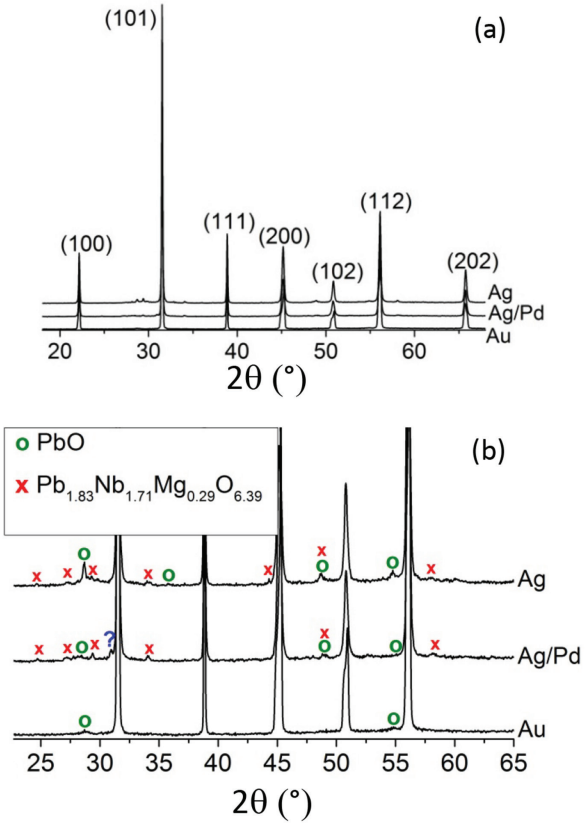

Figure 2: (a) XRD patterns of PMN–35PT thick films on Ag-, Ag/Pd- and Au-metalized substrates. The indexed peaks of the pseudo-cubic perovskite phase are shown in brackets (JCPDS 81-0861). (b) An enlarged 2θ-region from 23 to 65°. The peaks corresponding to PbO (JCPDS 78-1664) and pyrochlore $Pb_{1.83}Nb_{1.71}Mg_{0.29}O_{6.39}$ (JCPDS 33-0769) are marked by ***o*** and ***x***, respectively. The reflection, which cannot be clearly identified by crystallographic cards, is marked by a question mark in Fig. (b).

In addition to the perovskite reflections, also low-intensity PbO and pyrochlore reflections are observed in XRD patterns of the films on Ag- and Ag/Pd-metalized substrates. In the latter, also one reflection exists, which cannot be clearly identified by crystallographic cards in JCPDS base (marked by a question mark in Figure 2(b)). Note that the penetration depth of X-rays in PMN–35PT thick films is around 10 µm [10] and therefore the results show only the composition of the upper part of the thick films. On the other hand in the XRD pattern of PMN–35PT thick film on Au-metalized substrate the perovskite reflections and only a trace of two reflections corresponding to PbO phase can be observed. These low-intensity diffraction peaks are most probably related to the initial excess of PbO in the starting powder mixture (see Experimental methods). The secondary phases determined from the XRD patterns together with the dielectric properties of PMN–35PT thick films on metalized substrates are collected in Table 1.

Table 1: The secondary phases (SP) determined from the XRD patterns, the room-temperature dielectric and piezoelectric properties of PMN–35PT thick films on metalized substrates.

electrode	SP	ε` at 10 kHz	tan δ at 10 kHz	d_{33} at 5.5 kV/mm
Ag	PbO, Py	250	/*	/
Ag/Pd	PbO, Py, UP	300	0.04	/
Au	traces of PbO	1050	0.04	120

/not possible to pole
/*not possible to measure at 10 kHz, tan δ is 0.06 at 100 kHz
UP-unidentified phase, Py-pyrochlore

The dielectric permittivity of the films on Au-metalized substrates is 1050 at 10 kHz, which is more than three times higher than in the films on Ag- and Ag/Pd-metalized substrates. The tan δ of films on Au- and Ag/Pd-metalized substrates are in the same range. For films on Ag-metalized substrates the tan δ at 10 kHz was not possible to measure. Low values of ε` (i.e. 235) were previously reported also for PZT films on Ag/Pd-metalized LTCC (with no barrier layer between the LTCC and the electrode layer), which was attributed to intense interactions between the functional film and the substrate [14]. Furthermore, we were able to pole only the films on Au-metalized substrates (Table 1). The measured d_{33} coefficient of such films is 120 pC/N. Due to the superior phase purity, dielectric properties and ability of poling, we further analysed only the PMN–35PT films on Au-metalized (gilded) substrate. The microstructural, dielectric properties as a function of temperature and piezoelectric properties of these films are further discussed below.

3.3 The PMN–35PT thick films on gilded substrates

The photo of a PMN–35PT thick film on the gilded substrate is shown in Figure 3(a). The thick film surface is crack-free on cm scale. The BE-SEM images of the surface and polished cross-section of the film are shown

in Figure 3(b) and (c), respectively. Fig. 3(b) reveals a porous, but uniform microstructure. The estimated average grain size is ~0.8 µm. Some PbO, seen as a white inclusion in Figure 3(b), is also present in the film. The

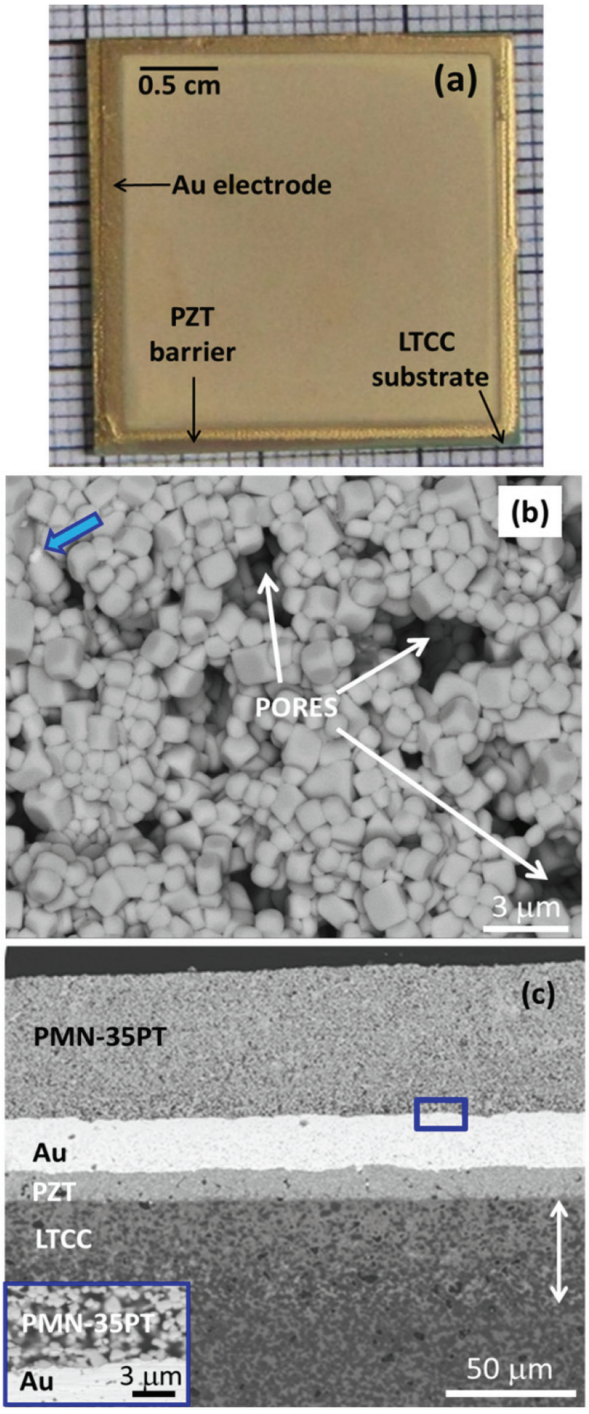

Figure 3: (a) The photo and BE-SEM images of (b) thick film surface and (c) polished cross-section of PMN–35PT thick film on gilded substrate. The thick arrow in panel (b) marks the PbO phase. In panel (c) the extension of a Pb rich layer in the LTCC is marked by an arrow and the inset shows an enlarged view of the PMN–35PT/Au interface.

results are in accordance with the XRD analysis, where in addition to the perovskite phase, a trace amount of PbO phase was also detected (see Fig. 2(b)). As seen in Figure 3(c) the thicknesses of the PZT barrier layer, Au and PMN–35PT film are ~15, ~25 and ~60 µm, respectively. The thickness of the PMN–35PT film is quite homogeneous across the substrate. No secondary phases are observed at the PMN–35PT/Au interface (inset in Figure 3(c)). Below the PZT layer into the LTCC substrate, a ~50 µm thick, brighter layer is formed (marked with an arrow). According to the EDXS analysis, this layer is PbO-rich and can be attributed to diffusion of PbO from PZT into the LTCC. Such layer was previously reported also in PZT/Au/LTCC structures, where the PbO diffused from the PZT functional layer into the substrate [13].

In Figure 4 the ε` and tan δ as a function of temperature are shown for the PMN–35PT thick film on gilded substrate. At 30 °C and 1 kHz the ε` and tan δ are 1150 and 0.06, respectively. The temperature of $\varepsilon`_{max}$ (~4800) at 1 kHz is 166 °C ± 1 °C, which is in agreement with the previously published temperature for PMN–35PT bulk ceramics [18, 19]. The ε` at room temperature is approximately three times lower than the one of the films on platinized alumina [7, 8] and approximately four times lower than PMN–35PT bulk ceramics [20], which could be attributed to the higher porosity and smaller average grain size of studied films on gilded LTCC substrates. On the other hand, the prepared films exhibit at least two times higher ε` at room temperature than previously published PZT films on LTCC substrates [12-14].

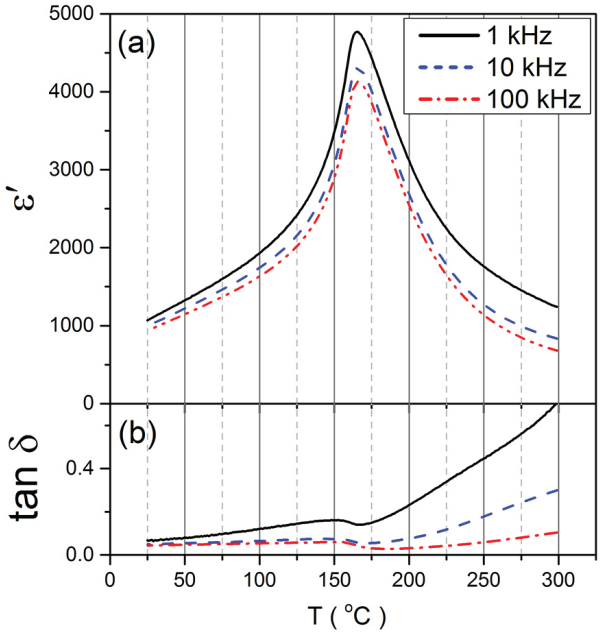

Figure 4: (a) ε′ and (b) tan δ of the PMN–35PT film on gilded substrate as a function of temperature at 1, 10 and 100 kHz.

Further the local piezoelectric response and ferroelectric domain configuration were investigated. The topography and out-of-plane PFM amplitude images are shown in Figure 5 (a) and (b), respectively. In the topographical image, the grain boundaries can be clearly identified, while in the amplitude image the grain boundaries are visible as dark non-active boundaries. The enhanced local piezoelectric activity is evident as brighter areas within the grains. An example of such region is marked by no. 1 in Figure 5 (b). The most frequently observed domains in the film are irregularly shaped domains found also in $Pb(Sc_{0.5}Nb_{0.5})O_3$ [21]. The size of the domains varies from a few hundred nanometres to a micrometre. Examples of such irregularly shaped domains are marked by thick arrows in Figure 5 (b). In addition rear lamellar-like domains can be found (marked by a thin arrow). Irregularly shaped and lamellar domains were previously observed also in PMN–35PT films on alumina substrates [22]. The local PFM amplitude and phase hysteresis loops are shown in Figure 5 (c) confirming a typical hysteretic response of the ferroelectric material and indicating the local domain switching.

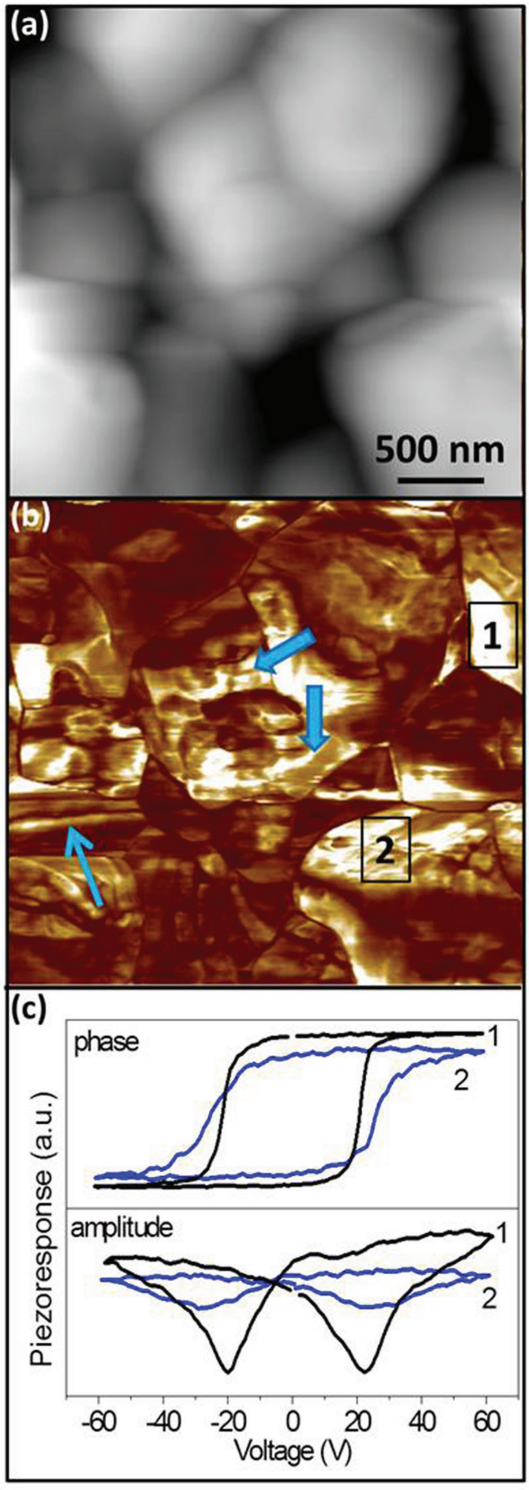

Figure 5: (a) Topography and (b) out-of-plane PFM amplitude image of the PMN–35PT thick film on gilded substrate. (c) PFM amplitude and phase hysteresis loops obtained from the areas marked by no. 1, 2 in the panel (b).

The PMN–35PT thick films were poled with a dc electric field of 2.5–7.5 kV/mm as described in Experimental section. The d_{33} values are collected in Table 2. For the films poled at 2.5 kV/mm, the d_{33} was 65 pC/N, but it increased with the increasing poling field until 5.5 kV/mm. The highest d_{33} of 120 pC/N was measured for the samples poled at electric field amplitudes between 5.5 and 7.5 kV/mm. The d_{33} coefficient is only 20 % lower than the one reported for PMN–35PT films on platinized alumina, i.e., ~150 pC/N for similar film thickness [10]. We note that the reduction of d_{33} in PZT thick films deposited on LTCC or on alumina was much more pronounced than in our PMN-PT films; i.e., 75 pC/N versus 125 pC/N, which is about 40 %. Such strong deterioration of the piezoelectric response was attributed to the interaction between the PZT film and the LTCC substrate [13]. It is also important to mentioned that the piezoelectric coefficient of PMN–35PT bulk ceramics prepared from the mechanochemically synthesized powder, but sintered at 1200 °C is ~640 pC/N (at similar poling conditions; electric field of 4.5 kV/mm) [20].

Table 2: The piezoelectric coefficient d_{33} measured for the PMN–35PT films poled at different electric field amplitudes.

Epoling (kV/mm)	d_{33} (pC/N)
2.5	65
3.5	85
4.5	100
5.5	120
6.5	120
7.5	120

The degradation of dielectric and piezoelectric properties of the PMN–35PT films on metalized LTCC substrates in comparison to the properties of the films on metalized alumina substrates could be related to the higher porosity of the films deposited on the former substrates. Further work is thus needed to improve the densification of the films on LTCC substrates.

4 Summary and conclusions

The compatibility of piezoelectric PMN–35PT thick-films with metalized LTCC substrates (DuPont 951) was studied. Three different bottom electrodes were used; Ag, Ag/Pd and Au. The XRD analysis revealed the presence of a large amount of secondary phases in the films prepared on Ag- and Ag/Pd-metalized substrates, while in the film deposited on the Au-metalized substrate only a trace of PbO phase was detected. Furthermore, about three times higher room temperature dielectric permittivity (1050 at 10 kHz) was measured in the films on Au- in comparison to the ones on Ag- and Ag/Pd-metalized substrates. The films on Ag- and Ag/Pd-metalized substrates could not be poled, but the ones on gilded substrates exhibit the piezoelectric coefficient d_{33} as high as 120 pC/N. Irregularly-shaped and lamellar-like domains with the size from a few hundred nanometres to micrometres were observed and the domain switching was confirmed by piezo-response force microscopy.

In conclusion, we succeeded to prepare ~60 μm thick PMN–35PT films on gilded substrates, where no film-substrate interactions were observed by SEM. The films exhibit high piezoelectric properties, much higher than the ones previously published for lead-based thick films on LTCCs. However, further work is needed to improve the densification of these films aiming to further enhance their functional properties.

5 Acknowledgements

This work was funded by M-ERA.NET project "*Integrated sensors with microfluidic features using LTCC Technology*" INTCERSEN (PR-06211) and the Slovenian Research Agency (research core funding No. P2-0105). Technical support by Mitja Jerlah, Jena Cilenšek, Brigita Kmet, Aneja Tuljak and Mateo Markov (*Erasmus+* program) is gratefully acknowledged.

6 References

1. Zarnik M S, Ursic H, Kosec M. Recent progress in thick-film piezoelectric actuators prepared by screen-printing, in: Piezoelectric Actuators *(open access)*, J. E. Segel, Ed., Nova Science Publishers Inc., 2011. https://www.novapublishers.com/catalog/product_info.php?products_id=30015
2. Imanaka Y. Multilayered low temperature cofired ceramics (LTCC) technology. New York, USA, Springer, 2005. http://link.springer.com/book/10.1007%2Fb101196
3. Makarovic K, Meden A, Hrovat M, Holc J, Bencan A, Dakskobler A, Kosec M. The effect of processing conditions on the properties of LTCC material, *J. Am. Ceram. Soc.*, 2012; 95: 760–767. http://onlinelibrary.wiley.com/doi/10.1111/j.1551-2916.2011.05027.x/abstract
4. Belavic D, Hrovat M, Zarnik MS, Holc J, Kosec M. An investigation of thick PZT films for sensor applications: A case study with different electrode materials, *J. Electroceram.*, 2009; 23: 1–5. http://link.springer.com/article/10.1007/s10832-008-9495-1
5. Singh A K, Pandey D. Evidence for MB and MC phases in the morphotropic phase boundary region of (1-x)[$Pb(Mg_{1/3}Nb_{2/3})O_3$]–x$PbTiO_3$: A rietveld study, *Phys. Rev. B*, 2003; 67, 064102 1–12. https://journals.aps.org/prb/pdf/10.1103/PhysRevB.67.064102
6. Handbook of Advanced Dielectric, Piezoelectric and Ferroelectric Materials, Z.-G. Ye, Ed. Cambridge, England, Woodhead Publishing Ltd, 1st ed., 2008. http://www.sciencedirect.com/science/book/9781845691868
7. Ursic H, Hrovat M, Holc J, Tellier J, Drnovsek S, Guiblin N, Dkhil B, Kosec M. Influence of the substrate on the phase composition and electrical properties of 0.65PMN–0.35PT thick films, *J. Eur. Ceram. Soc.*, 2010; 30: 2081–2092. http://www.sciencedirect.com/science/article/pii/S0955221910001615
8. Gentil S, Damjanovic D, Setter N. Development of relaxor ferroelectric materials for screen-printing on alumina and silicon substrates. *J. Eur. Ceram. Soc.*, 2005; 25: 2125–2128. http://www.sciencedirect.com/science/article/pii/S095522190500169X
9. Gentil S, Damjanovic D, Setter N. $Pb(Mg_{1/3}Nb_{2/3})O_3$ and (1-x)$Pb(Mg_{1/3}Nb_{2/3})O_3$–x$PbTiO_3$ relaxor ferroelectric thick films: processing and electrical characterization. *J. Electroceram.,* 2004*;* 12: 151–161. http://link.springer.com/article/10.1023/B:JECR.0000037720.39443.e3
10. Ursic H, Zarnik, MS, Tellier J, Hrovat M, Holc J, Kosec M. The influence of thermal stresses on the phase composition of 0.65$Pb(Mg_{1/3}Nb_{2/3})O_3$–0.35$PbTiO_3$ thick films, *J. Appl. Phys.*, 2011; 109: 014101 1–5. http://aip.scitation.org/doi/full/10.1063/1.3526971
11. Ursic H, Zarnik MS, Kosec M. $Pb(Mg_{1/3}Nb_{2/3})O_3$–$PbTiO_3$ (PMN–PT) material for actuator applications, *Smart Materials Research (open access),*

2011; 2011: 452901 1–6. https://www.hindawi.com/journals/smr/2011/452901/

12. Hrovat M, Holc J, Drnovsek S, Belavic D, Cilensek J, Kosec M. PZT thick films on LTCC substrates with an interposed alumina barrier layer, *J. Eur. Ceram. Soc.,* 2006; 26: 897–900. http://www.sciencedirect.com/science/article/pii/S0955221905000634
13. Ursic H, Hrovat M, Belavic D, Cilensek J, Drnovsek S, Holc J, Zarnik MS, Kosec M. Microstructural and electrical characterisation of PZT thick films on LTCC substrates, *J. Eur. Ceram. Soc.*, 2008; 28: 1839–1844. http://www.sciencedirect.com/science/article/pii/S0955221908000253
14. Golonka L J, Buczek M, Hrovat M, Belavic D, Dziedzic A, Roguszczak H, Zawada T, Properties of PZT thick films made on LTCC, *Microelectronics Int*., 2005; 22: 13–16. http://www.emeraldinsight.com/doi/abs/10.1108/13565360510592171
15. Gebhardt S, Seffner L, Schlenkrich F, Schonecker A. PZT thick films for sensor and actuator applications, *J. Eur. Ceram. Soc.*, 2007; 27: 4177–4180. http://www.sciencedirect.com/science/article/pii/S095522190700163X
16. Ursic H, Tchernychova E, Bencan A, Jouin J, Holc J, Drnovsek S, Hrovat M, Malic B. The influence of the platinum substrate roughness on the ferroelectric properties of 0.65Pb($Mg_{1/3}Nb_{2/3}$)O_3–0.35$PbTiO_3$ thick films, Informacije MIDEM, *Journal of Microelectronics, Electronic Components and Materials (open access)*, 2014; 44: 12–18, http://www.midem-drustvo.si/Journal%20papers/MIDEM_44(2014)1p12.pdf
17. Holc J, Hrovat M, Kosec M. Interactions between alumina and PLZT thick films. *Mater. Res. Bull.,* 1999; 34: 2271–8. http://www.sciencedirect.com/science/article/pii/S0025540899002275
18. Alguero M, Ricote J, Jimenez R., Ramos P, Carreaud J, Dkhil B, Kiat J M, Holc J, Kosec M. Size effect in morphotropic phase boundary Pb ($Mg_{1/3}Nb_{2/3}$)O_3–$PbTiO_3$, *Appl. Phys. Lett*., 2007; 91: 112905 1–3. http://aip.scitation.org/doi/abs/10.1063/1.2778471
19. Leite E R, Scotch A M, Khan A, Li T, Chan H M, Harmer M P, Liu S F and Park S E. Chemical heterogeneity in PMN–35PT ceramics and effects on dielectric and piezoelectric properties, *J. Am. Ceram. Soc.*, 2002; 85: 3018–3024. http://onlinelibrary.wiley.com/doi/10.1111/j.1151-2916.2002.tb00572.x/abstract
20. Ursic H, Tellier J, Hrovat M, Holc J, Drnovsek S, Bobnar V, Alguero M, Kosec M. The Effect of Poling on the Properties of 0.65Pb($Mg_{1/3}Nb_{2/3}$)O_3–0.35$PbTiO_3$ Ceramics, *Jpn. J. Appl. Phys.*, 2011; 50: 035801-6.
21. Ursic H, Drnovsek S, Malic B. Complex domain structure in polycrystalline Pb($Sc_{0.5}Nb_{0.5}$)O_3, *J. Phys .D: Appl. Phys.,* 2016**;** 49: 115304 1–4. http://iopscience.iop.org/article/10.1088/0022-3727/49/11/115304
22. Ursic H, Ricote J, Amorin H, Holc J, Alguero M. Ferroelectric domain configurations in 0.65Pb($Mg_{1/3}Nb_{2/3}$)O_3–0.35$PbTiO_3$ thick films determined by piezoresponse force microscopy, *J. Phys. D: Appl. Phys.*, 2012; 45: 265402 1–11. http://iopscience.iop.org/article/10.1088/0022-3727/45/26/265402

Arrived: 17. 04. 2017
Accepted: 13. 07. 2017